OXFORD UNIVERSITY PRESS | Cerebral Cortex

Global coding in rat barrel cortex in the absence of local cues

Journal:	*Cerebral Cortex*
Manuscript ID	CerCor-2016-01628.R1
Manuscript Type:	Original Articles
Date Submitted by the Author:	n/a
Complete List of Authors:	Gerdjikov, Todor; University of Leicester, Department of Neuroscience, Psychology and Behaviour Bergner, Caroline; Universitatsklinikum Gottingen, Department for Neurology Schwarz, Cornelius; Hertie Institute for Clinical Brain Research, Department for Cognitive Neurology
Keywords:	head-fixed rat, neuronal coding, primary somatosensory cortex, discrimination psychophysics, tactile perception

GLOBAL TACTILE CODING IN RAT BARREL CORTEX IN THE ABSENCE OF LOCAL CUES

Todor V. Gerdjikov[1,2,3] Caroline G. Bergner[1,2], Cornelius Schwarz[1,2*]

[1] Werner Reichardt Center for Integrative Neuroscience, Systems Neuroscience, Eberhard Karls University, Tübingen, Germany
[2] Hertie Institute for Clinical Brain Research, Dept. Cognitive Neurology, Eberhard Karls University, Tübingen, Germany
[3] Department of Neuroscience, Psychology and Behaviour, University of Leicester, Leicester, UK

Abbreviated title: Global coding in barrel cortex

33 pages, 7 figures.
Word counts:

Abstract	184
Introduction	560
Discussion	1878

* Correspondence: Cornelius Schwarz
Werner Reichardt Center for Integrative Neuroscience
Systems Neurophysiology
University Tübingen
Otfried Müller Str. 25
72076 Tübingen, Germany
Phone: +49 7071 2980462
Fax: +49 7071 295724
email: cornelius.schwarz@uni-tuebingen.de

Keywords: head-fixed rat, neuronal coding, primary somatosensory cortex, discrimination psychophysics, tactile perception

Funding: This research was supported by grants from the Deutsche Forschungsgemeinschaft (DFG SCHW 577/10-2 and DFG SCHW 577/14-1 to C.S.). T.V.G. was initially supported by a postdoctoral fellowship from the Hertie Foundation. C.G.B. was supported by a stipend from IZKF Medical School University Tübingen.

Notes: We thank Ursula Pascht for excellent technical assistance. Conflicts of interest: None declared.

Abstract

While whisker-related perception is based predominantly on local, near-instantaneous coding, global, intensive coding, which integrates the vibrotactile signal over time, has also been shown to play a role given appropriate behavioral conditions. Here we study global coding in isolation by studying head-fixed rats that identified pulsatile stimuli differing in pulse frequency but not in pulse waveforms, thus abolishing perception based on local coding. We quantified time-locking and spike counts as likely variables underpinning the two coding schemes. Both neurometric variables contained substantial stimulus information, carried even by spikes of single barrel cortex neurons. To elucidate which type of information is actually used by the rats, we systematically compared psychometric with neurometric sensitivity based on the two coding schemes. Neurometric performance was calculated by using a population-encoding model incorporating the properties of our recorded neuron sample. We found that sensitivity calculated from spike counts sampled over long periods (> 1 s) matched the performance of rats better than the one carried by spikes time-locked to the stimulus. We conclude that spike counts are more relevant to tactile perception when instantaneous kinematic parameters are not available.

Introduction

Texture perception is based on skin/hair vibrations evoked by their relative movement against an object. Unlike vision, in which the percept describes a highly structured visual scene, and thus local features are considered to carry significant sensory information, texture identification is traditionally thought to be based on a broad-band input signal mirroring texture surface. For this reason classic studies of texture perception have largely been focused on 'global' aspects of tactile coding, also called 'intensive coding' (LaMotte and Mountcastle 1975; Lederman 1982; Yoshioka et al. 2001) while in vision 'local' features such as edges have drawn much more attention (Marr 1982). A novel concept, called slip or waveform coding, incorporates the fact that a sensor moving against an object is a frictional system and generates stick-slip movements (Jadhav and Feldman 2010; Schwarz 2016). In fact these slips contain a wealth of texture information (Wolfe et al. 2008) and are local features in space and time, which have the potential to bring concepts of tactile perception closer to the ones known from vision - with the difference that local slip features may occur in a more stochastic fashion, while visual local features are fixed at a defined point in space-time. There is accumulating support for local encoding in the tactile sense, such as high resolution coding (Johansson and Birznieks 2004; Stüttgen and Schwarz 2010; Mackevicius et al. 2012; Chagas et al. 2013), temporally local, i.e. instantaneous coding (Arabzadeh et al. 2005; Jadhav et al. 2009; Waiblinger, Brugger, and Schwarz 2015; Waiblinger, Brugger, Whitmire, et al. 2015), and spatially local coding (Hayward et al. 2014; Jörntell et al. 2014; Delhaye et al. 2016).

In the rat whisker system studied here, direct comparison of local vs. global coding schemes show the tactile percept to be strongly dominated by local features (Waiblinger, Brugger, and Schwarz 2015; Waiblinger, Brugger, Whitmire, et al. 2015). However, when exposed to stimuli devoid of local cues, rats show a capacity for global stimulus encoding (Gerdjikov et al. 2010; Georgieva et al. 2014; Waiblinger, Brugger, and Schwarz 2015). Thus, there is reason to believe that local as well as global cues gain access to the tactile perceptional

system. Classically, two major variants of global coding schemes have been considered, 'frequency' and 'intensity' (LaMotte and Mountcastle 1975). Frequency is thought to exploit a characteristic of the spectrum of the vibrotactile signal, while intensity calculates some form of signal average. While local features in the vibrotactile waveform are extracted by precise time-locked spiking of neurons on the ascending tactile pathway (Jadhav et al. 2009; Chagas et al. 2013), the neuronal code capturing global variables has remained unclear.

Here we studied tactile discrimination using passively applied pulsatile tactile stimuli in head-fixed rats. Discriminanda were presented in a controlled fashion and consisted of repetitive, identical pulse waveforms that contained stimulus information exclusively in the timing of individual pulses. In this way local cues were absent and subjects were forced to base their decision on intensive coding, i.e. either intensity or frequency. We compared barrel cortex unit activity recorded in the barrel column receiving signals from the deflected whisker (C1) with the discrimination performance of the animal. Our results show that in the absence of instantaneous coding, the psychophysical performance best fits integration of firing rate of primary cortex over long time segments (> 1 s), rather than using spikes times locked to stimulus features.

Methods

The spike data recorded in this study was collected from operantly conditioned rats performing a tactile discrimination task. The behavior has been reported in Gerdjikov et al. (2010). Behavioral methods are thus identical to the previous report. In brief, three male Sprague Dawley rats (weight, 250-350g; Harlan Winkelmann, Borchen, Germany) were housed together on a 12 h reversed light–dark cycle (lights on at 8 pm) at a temperature of 22-24°C, relative humidity 55%. Food was always freely available. Water was freely available until the start of behavioral testing. Rats were handled for about 5 min every day for two consecutive weeks after arrival. All animals were treated in full compliance with the German Law for the Protection of Animals.

Surgery

To prevent infection, antibiotic solution (Baytril, Bayer HealthCare AG, Leverkusen, Germany) was added to the drinking water (0.2 mg/ml) for 3 days before and 7 days following surgery. Rats were anesthetized in an induction chamber using a volatile anesthetic (5% isoflurane; Abbott GmbH, Wiesbaden, Germany) mixed with oxygen in a vaporizer system (Drägerwerk AG, Lübeck Germany). Body temperature was monitored rectally and maintained at 37 Cº using a homoeothermic pad. For fluid replacement, 5% glucose was administered subcutaneously at regular intervals (5 ml total injection volume). Anesthetized animals were fitted to a stereotaxic apparatus and isoflurane was administered at a concentration needed to maintain anesthesia (typically around 1%). After shaving and disinfection the skin was incised and the pericranium retracted. Stainless steel screws fitted into pre-drilled holes in the skull served as anchors for a head-mount formed from light-curing dental composite (Heliomolar Flow, Ivoclar Vivadent AG, Schaan, Lichtenstein). Craniotomy was performed over barrel cortex and the C1 column was located by mapping the cortex with a single intracerebral electrode. A 2 x 2 multielectrode array (inter-electrode distance ≈ 250 mm) was slowly inserted into the identified location of the C1 column and fixed to the head-mount with dental polymer. A 5 X 25 mm screw was embedded upside

down to serve as a head-post. Nebacetin antibiotic ointment (Yamanouchi Pharma GmbH, Heidelberg, Germany) was applied before closing the skin with sutures. For analgesia, buprenorphine hydrochloride in solution (0.1 mg/kg; Reckitt Benckiser, Hull, UK) was injected immediately after surgery and twice daily on three consecutive days postoperatively. Rats were housed singly after surgery and were given 3 weeks of recovery before the start of behavioral testing. Handling resumed one week postoperatively and continued throughout the duration of the experiment.

Stimuli, apparatus, and behavioral procedures

A glass capillary mounted on a piezo bender was used to apply pulsatile deflections to the left whisker C1. The pulses were all identical having the shape of a single-period sine wave (100 Hz, duration 10 ms, amplitude 11.3°, rostral direction) presented for 5 s at inter-pulse intervals of 11.1 to 66.7 ms corresponding to frequencies of 15 to 90 Hz (Fig. 1A). The frequency spectrum of these pulsatile stimuli is characterized by a fundamental frequency (=pulse frequency), and several harmonics. More than 99% of the power is contained in frequencies up to 150 Hz. The fraction of total power contained in the fundamental frequency is smallest at 15 Hz (with many harmonics) and largest at 90 Hz (with pulse duration of 10 ms and period of 11.1 ms close to a sinusoid). Changes in pulse frequency would alter the number of harmonics, while changes in pulse amplitude just changes total power keeping the spectrum's shape. A maximum difference of 3% in pulse amplitude and peak velocity when presented with pulse frequencies between 15 to 90 Hz was measured using a modified photodiode (Stüttgen et al. 2006). The capillary tip was positioned 5 mm away from the skin and tilted at an angle of 155 to 175° against the whisker. Rats earned water rewards by licking at a spout positioned in front of their mouth.

Rat handling, habituation, water control, and monitoring of licking movements were done exactly as described in a previous review (Schwarz et al. 2010). Behavioral testing was done in a quiet environment (foam padded, vented behavioral box, volume 1 m^3). Sound emission of the piezo benders were dampened by fitting earplugs (Oropax, Wehrheim, Germany), and

masked by a constant white background noise (70 dB, generated by an arbitrary waveform generator, W&R Systems, Vienna, Austria). None of the animals responded consistently in control sessions identical to experimental sessions, except that the whisker was detached from the stimulator. This ensured that non-tactile cues did not play a role in their performance. During water control body weight was monitored daily to ensure normal growth.

Psychophysical testing was conducted using the method of constant stimuli. Stimuli were always presented in blocks of ten. Stimulus order was chosen randomly within each block and across blocks. One block consisted of five rewarded stimuli at 90 Hz and five non-rewarded stimuli, each presented for 5 s. The inter-trial period varied between 15-25 s. Licking in a prestimulus period led to a time out of 10 s.

Electrophysiology

Movable multi-electrode arrays (impedance 2-6 MΩ) were manufactured in-house from quartz-coated, pulled and ground platinum/tungsten microelectrode fiber (Thomas Recording, Giessen, Germany) (Haiss et al. 2010). Electrode depth could be adjusted by turning an M1 microscrew (250 µm per full revolution). The array was lowered prior to each recording session by one quarter turn or more as needed to identify spikes, and stayed in this location until the next session. Voltage traces were bandpass-filtered (200-5000 Hz) and recorded continuously at a sampling rate of 20 kHz using a multichannel extracellular amplifier (Multi Channel Systems, Reutlingen, Germany). Spikes were extracted offline using amplitude thresholds. Spike waveforms (duration 2 ms) centered on the time bin, in which the voltage trace first traversed the amplitude threshold, were subjected to an independent component analysis to remove electrode cross-talk and sorted using a custom-written program based on Kohonen maps (Hermle et al. 2004). Single unit classification was based on criteria derived from waveform statistics as previously described (Möck et al. 2006).

Data analysis

Psychophysical data assessed as response probabilities was converted into sensitivity d' using

$$d' = \Phi^{-1}p_{HIT} - \Phi^{-1}p_{FA} \quad \text{Eq. 1}$$

where Φ signifies the probit function, p_{HIT} signifies the probability of correct responses, and p_{FA} the probability of false alarms (Stüttgen and Schwarz 2008). In order to compare psychometric with neurometric sensitivities d' values were converted to area under the receiver operating curve (AUC) (Stanislaw and Todorov 1999)

$$AUC = \frac{\Phi(d')}{\sqrt{2}} \quad \text{Eq. 2}$$

which corresponds to the percentage correct responses of an unbiased, ideal observer under the conditions of a two alternative forced choice procedure (Green and Swets 1966; Stüttgen et al. 2011). Neuronal sensitivities were computed for two possible coding symbols: spike count and best frequency. Spike count is the number of spikes found in a time interval. Best frequency was determined by maximizing the power spectral density of the PSTH obtained in the 5s stimulus interval. AUC was calculated for pairs of coding symbol distributions acquired with one S- (15-75 Hz) and the S+ (90 Hz). Error bars of psychometric data in this study signify 95% confidence intervals calculated from a binomial model setting the animal's response probability to the probability of a Bernoulli trial. All calculations were done in Matlab (MathWorks, Natick, MA).

Pulse locking was assessed as vector strength defined by (Batschelet 1981):

$$v = \frac{1}{n}\sqrt{(\sum \sin(a_i))^2 + (\sum \cos(a_i))^2} \quad \text{Eq. 3}$$

where a_i is the phase angle of spike occurrence i relative to stimulus period (over all stimulus trains), and n is the total number of spike occurrences. The length of the period for the calculation of vector strength was defined as the time windows between the onset of

subsequent pulses (ranging between 66.7 ms for 15 Hz and 11.1 ms for 90 Hz). The significance of vector strength was assessed with the Rayleigh test for non-uniformity ($p<0.05$; Fisher, 1995). The vector strength of pulsatile stimuli is not constant across different pulse frequencies, because the pulse waveform fills the inter-pulse period differently (cf. Figs. 4 and 5). Therefore, a spike response, perfectly time-locked to the pulse onset, would artificially lead to decreasing vector strength with higher frequencies. We coped with this by calculating normalized vector strengths. The vector strength obtained with each frequency was normalized to the one calculated using the spike response to the 15 Hz stimulus, but cutting the inter-pulse period to that of the respective stimulus (e.g. the vector strength of spiking observed with 30 Hz would be divided by the vector strength obtained with 15 Hz but assuming an inter-pulse period of 33.3 ms, thus omitting all spikes that occurred later in the 15 Hz inter-pulse period).

To directly compare spike timing with spike count coding, we formed neuronal pools of various sizes (3-160) and composition (10-80 best responding neurons). For spike timing, best responding neurons were sampled with replacement from neurons showing the highest vector strength during 60Hz stimulation. However, for the model we did not use pulse locking, because it is a variable that is not accessible for the animal (without prior knowledge of stimulus frequency). Instead we used spectral analysis which in principle the animal could use. For each unit in the pool we generated a spike train based on spiking probabilities derived from the unit's actual PSTH. Denoting the firing probability in each 1 ms bin by p, we generated a random number r from a uniform probability distribution within the interval [0 1] and assigned a spike for that bin if $r > 1 - p$. We summed these synthetic spike trains into a population PSTH for each neuronal pool and found the peak of the PSTH power spectrum (Welch spectrum with a 256 sample Hanning window). This process was repeated 1000 times to arrive at discrete parameter distributions. AUC values were computed from these distributions as done with experimental data.

Spike count-based calculations were carried out in an identical manner except that (i) neurons were ranked based on firing rates (rather than vector strength) during stimulation at 60 Hz and (ii) AUC calculations were based on number of spikes/stimulus as contained in the population PSTH (rather than peak of the PSTH power spectrum).

The count-based rank order mirrors also the generation of excess spikes in response to the stimulus, as the baseline-subtracted firing rate shows a high correlation with excess spikes ($r = 0.92$, $p < 0.001$). For vector-based ranking this was not the case (correlation between vector strength and excess spikes: $r=0.01$, $p=0.90$). Quantitative comparison of psychometric and neurometric curves was done by calculating the Euclidean distance between them.

Results

We analyzed spike activity recorded in barrel cortex of rats while the animals performed a tactile discrimination task [the behavioral results were published in (Gerdjikov et al. 2010)]. Head-fixed rats were trained to report in a Go/NoGo task, whether pulsatile deflections of whisker C1 at different pulse frequencies would (S+: 90 Hz) or would not (S-: 15, 30, 45, 60, 75 Hz) predict reward. To facilitate temporal integration, and to suppress impulsive responding, the animals were trained to wait for 4.5 s after stimulus onset (total stimulus duration 5 s) before licking a water spout to obtain reward (Fig. 1A). All stimulus pulses had an identical shape (one period cosine waveform of 10 ms duration and 11.3° amplitude), thus the only strategy allowing discrimination was temporal integration over a series of subsequent pulses (cf. Waiblinger et al., 2015a). The ability of the rat to discriminate between pairs of stimuli, called psychometric sensitivity, was expressed as the area under curve (AUC), an estimate derived from ideal observer analysis (see methods). AUC estimates the probability of the rat observer to discriminate one stimulus against another. Rats achieved a sensitivity of 0.58 for the most difficult comparison (90 vs. 75 Hz), which monotonically increased to 0.85 for the most easy discrimination (90 vs 15 Hz) (Fig. 1BC). In the following we will describe how pulsatile stimuli are represented by principal barrel column neurons in the behaving rat. We will then focus on two prominent candidates of neuronal coding symbols, best frequency and spike counts. These variables will then be converted to AUC neurometric sensitivity values to quantitatively compare neurometric with psychometric performance and derive arguments about the neuronal coding scheme the animals used to solve the task.

Spike counts

The single units presented in this study (N = 80) were sampled from the principal barrel column of the stimulated whisker C1, across all layers, in three animals performing the psychophysical task (units/sessions per animal: 35/17, 35/20, 10/5). Figure 2A shows spike recordings from three example neurons (excited, non-responsive and inhibited). Raster

displays (top) were converted into firing rates using 5 ms bins and plotted as peri-stimulus time histograms (PSTHs, center) and cumulative spike numbers (bottom). The latter were obtained by fitting a regression line to the baseline cumulative response and subtracting the obtained line from the cumulative response across the full recording period. Many neurons showed a clear onset response followed by either decay to spontaneous levels, or tonic excitation or inhibition. To illustrate the continuum of responses in the population, we first plotted the spontaneous firing rate against the evoked firing rate (the first obtained in the 4 s interval before stimulus onset: the latter in the 4 s interval before stimulus offset, excluding the on-response) (Fig. 2B). It can be appreciated that evoked spike counts do not reveal particularly salient neuronal responses. Predominantly neurons with lower spontaneous rates appear to generate additional stimulus driven spikes. The inhibited neurons do not stand out as a clearly defined cluster. To improve the presentation we constructed a 95% confidence interval from the baseline firing assuming that firing is governed by a Poisson process (Abeles 1982). Integrating the firing rate curve above or below these confidence limits and averaging across stimulus frequencies produced the average number of significant spikes evoked or suppressed by vibrotactile stimulation. These counts are called excess spikes whose distribution across all units (averaged across stimulation frequency) is shown in figure 2C (negative excess spikes = suppressed spikes). Here the tendency of low firing neurons to exceed positive excess spike rates and that of high firing neurons to generate negative excess spikes is more obvious. A major result here again is that a large majority of neurons do not respond to the stimulus when counting spikes in a long interval. This result is also reflected in the flat tuning curves shown by most of the neurons based on spike rates observed within the 5 seconds stimulus interval (Fig. 3A). The relative non-responsiveness of barrel cortex to long series of pulses (which is in stark contrast to tuning functions of primary afferents; cf. Gerdjikov et al., 2010) are partly due to the known strong frequency-dependent spike rate adaptation (Garabedian et al. 2003; Khatri et al. 2004; Melzer et al. 2006; Stüttgen and Schwarz 2010), which our single neuron data clearly confirm: The total

number of spikes per pulse (integrated over the 5 s of stimulation) decreased significantly across frequencies (Fig. 3B; χ^2= 368.08, df = 5, p < .001, Friedman's test, N = 80 neurons)

Pulse-locking

Next, we were interested in how the timing of spikes was related to stimulus pulses. To this end we constructed pulse triggered PSTHs and calculated the vector strength, which quantifies the degree of pulse locking by numbers ranging from 0 (random distribution of spikes) and 1 (all spikes accumulated in one phase bin) (Goldberg and Brown 1968). A note of caution needs to put forward here. A phase code is not a realistic coding symbol as the subject does not have prior knowledge of pulse frequency and phase. Therefore the analyses in this paragraph only serve to describe the properties of spike timing but do not bear on the animal's usage of this timing to reach a perceptual decision (cf. Fig. 7 where we used spectral analysis to model a neuronal pool's decision about a stimulus). Figure 4 demonstrates two neurons generating zero excess spikes in response to the pulsatile stimulus. Despite their unresponsiveness in terms of spike rate, the first neuron locked very well to the stimulus pulses as can be appreciated in the phase histograms. However, as demonstrated in the inset of figure 4 (neuron 1), despite precise locking, the percentage of pulses that actually evoke a spike may be very low. Neuron 2, in contrast, fired at a high rate, and displayed minor time-locking.

Next, we assessed the peak of spiking for each pulse phase histogram and plotted it as latency distribution (Fig. 5A; N=80 neurons). The quite narrowly peaked distribution right after the offset of the stimulus pulse reveals that spike timing relates to absolute onset times of pulses, and not to the phase of the pulse frequency. We therefore call precise spiking observed here 'time-locked' (rather than 'phase-locked'). Calculating the vector strength of the phase histograms for all responses obtained with the 15 Hz stimulus revealed that vector strength tends to be higher in units showing positive excess spikes as compared to units with negative excess spikes (Fig. 5B; Mann-Whitney U = 8477.00, p< .001, this was similarly the case for all pulse frequencies, not shown). It is worth to point out that 'non-responding'

cells (with near-zero excess spikes) often do convey stimulus information by time locking. In order to portray spike time-locking at higher stimulus frequencies, we aimed at arriving at a measure that would indicate to what extent time-locking survives higher frequency stimulation. The classical vector strength (Batschelet 1981) is not suited for this purpose, because it would decrease for shorter inter-pulse intervals even with stable time locking (that is exactly what was observed; results not shown). We therefore present a normalized version of vector strengths: The classical vector strength for each pulse frequency was related to the one obtained with 15 Hz stimulation, but considering only spikes falling into the range of the respective inter-pulse period. This normalized vector strength is expected to be one, if time-locking survives stimulation at higher pulse frequencies. In the population of units (N=80) we observe a large variety of normalized vector strength, but on average this expectation was met: The medians of the distributions are close to one. The normalized vector strengths of spike responses to 75 and 90 Hz tends to deviate from this expectation toward lower values - likely because time-locked spikes at these frequencies start to spill over into the next pulse period, and thus are omitted by the normalization procedure. In summary, time-locking spikes in a population of cells should be able to convey considerable information about pulse frequency.

The analyses presented so far suggest that both spike counts as well as spike locking convey significant information about pulse frequency (or stimulus intensity), and thus, may both explain the animals' behavioral performance. By quantitatively comparing these sources of information with the animals' performance, the next section deals with the question of which of these sources, or to which extent both of them, are used by the animals.

Comparing psychometric with neurometric sensitivity based on spike counts

To allow direct comparisons with behavioral sensitivity (Fig. 1C), neuronal sensitivities were estimated by calculating AUC (see methods). First we focus on neurometric estimates based on spike counts. AUC was calculated from spike count distributions in response to S+ and each of the S- stimuli in pairwise fashion. The three example neurons shown in figure 6A

show an increase in sensitivity with longer windows, most conspicuously for comparisons including lower frequency S-, but levelling off, or even descending with windows longer than ~2 s. Figure 6B visualizes the distribution of sensitivity across the total sample of neurons for the 5 different comparisons (5 panels) and different durations of integration windows (gray value of the lines). For comparison the psychometric data are rendered as well (black symbols, same as Fig. 1C). Psychometric and neurometric sensitivities decrease as the difference between comparison frequencies decreases (i.e with higher S- frequency). Further, neurometric sensitivity distributions obtained with longer window durations are shifted upward and show heavy tails toward higher AUC values. In contrast, very small windows containing just the transient ON-responses of many neurons did not yield higher AUC values (broken lines), suggesting that these transients, as prominent as they may feature in PSTHs (cf. Fig 2A), do not contain much information of pulse frequency. The psychometric sensitivity is located at the upper reaches of the neuronal AUC distributions, in line with the notion that the neurons with highest sensitivities may determine the animal's behavior. However, with all window sizes (except the on-response) there is a percentage of cells showing higher sensitivity than the animal.

In a final approach we aimed at a systematic appraisal of the goodness of fit of 'count-based' versus 'timing-based' neurometric sensitivity to the rats' performance. We explicitly wanted to consider the distribution of coding properties as found in our recorded sample of cells, and therefore strived to account for coding within a realistic population of barrel cortex neurons, reflecting properties found amongst our recorded sample. Therefore we resampled synthetic spike trains employing firing probabilities of subsets of recorded neurons, which were used to construct a population PSTH. In a Monte-Carlo fashion we varied the number of neurons contributing to the PSTH and the number of most sensitive neurons amongst which the members of that pool would be selected at random for each resampling step. It is important to emphasize that we refrained from basing the estimation of spike timing on vector strength because the animals do not have access to stimulus phase information. Instead we based the estimate of frequency coding on resampled distributions of best frequencies contained in

the power spectral density of the resampled population PSTHs. The results are shown in figure 7. Euclidean distances of psychometric and neurometric curves obtained with 10-80 best neurons and 3-160 neurons in the pool are plotted as color matrices. Locking-based sensitivities (bottom) maximally aligned to the rats' average psychometric performance with a lower number of input neurons (40 neurons sampled from 40 best units; turquoise band), but overall fared worse than count-based sensitivities (top) (blue area), which, even though requiring larger neuronal pools to reach their minima (120 neurons sampled from 60 best units) achieved a closer match to behavior across a large area of pool sizes and selected neurons. Three example comparisons of psycho- vs. neurometric curves (including the best fitting models, gray) are shown around the matrices. The relative mismatch of spike timing based curves was mainly due to their consistent outperformance of the rat observer with lower pulse frequencies (as suggested by superb time locking seen with these stimuli, cf. Figs. 4 and 5).

Discussion

This work investigated neuronal coding symbols in barrel cortex carrying information about so-called 'global' or 'intensive' tactile stimulus variables. The two relevant global variables are stimulus frequency and intensity and were separated from 'local', 'instantaneous', or 'waveform' variables using stimuli that varied the two global variables in conjunction while keeping local waveforms unchanged (Schwarz 2016). Two coding symbols were investigated, 'spike count' and 'stimulus-locked spike timing'. We found that both spike count and timing carry substantial stimulus information. A quantitative comparison of neurometric to psychometric sensitivities, however, clearly pointed to spike counts as the more relevant coding symbol.

Our experiment was designed to isolate global from local stimulus variables. An arising question then is, which of the global variables, frequency or intensity, is actually encoded? To control the role of the local waveform, we needed to use stimuli that contained the two global variables in a highly co-varying fashion. Thus, our present experiments cannot directly address this question. We will discuss the most likely associations of encoded stimulus variable and neuronal coding symbol in later paragraphs. We are well aware that previous studies, often implicitly, asserted unique solutions to the problem (e.g. LaMotte and Mountcastle, 1975; Arabzadeh et al., 2003; Harris et al., 2006; Adibi et al., 2012). However, any strict causal statement about the encoding of stimulus variables is prone to logical fallacy, if other hidden, correlated and contributing variables cannot be excluded. The present state of affairs is just this - the perceptually relevant, local variable has only recently been added to the group of contenders (Waiblinger, Brugger, and Schwarz 2015; Schwarz 2016). The three candidate variables, local waveform, intensity and frequency are entangled in a way that makes it impossible to design sinusoids that would vary one of them along a dimension orthogonal to the two others. Sine frequency concomitantly changes both intensity and local waveform, while intensity (i.e. sine amplitude) co-varies with local waveform. As arbitrary waveforms can be formulated as a linear superposition of sinusoids,

they will suffer from the same problem. One could hope to balance out elemental sinusoids to achieve orthogonality (with respect to two dimensions), however, it would probably require either reducing the usable parametric range, or limiting stimulus duration. It is thus a task for future studies to come up with broadband stimulus designs that allow to do meaningful experiments and to control two variables at a time. The pulsatile stimuli used here, in a way, cover middle ground. They allow the separation of one of the three variables at a time. In practical terms, they work for our purposes, because firstly, they allow a very specific and easy access to control local waveform, the dominant perceptual variable (Waiblinger, Brugger, and Schwarz 2015). This property is very convenient as it separates local from global variables in a straight forward way, by simply keeping pulse waveform constant. Secondly, pulsatile stimuli work for us, because we can ignore the full spectral impact of changing any variable, that is we substitute the variable 'frequency' (containing the full spectral content) by the fundamental frequency found in the spectrum (equal to pulse frequency). Ignoring the rather complex spectral characteristics (see methods) is justified by the fact that previous experiments showed that they are perceptually irrelevant: Psychometric curves obtained from stimuli keeping either pulse frequency or amplitude constant (while changing the respective other) are identical (Waiblinger et al., 2015a, cf. their Fig. 2A).

Our results support the notion that spike counts are relevant coding symbol used to convey information about tactile global stimulus variables. It has been the traditional coding symbol used to study various coding problems from visual motion (Britten et al. 1992) loudness (Micheyl et al. 2013) to tactile frequency (Mountcastle et al. 1969; Luna et al. 2005). The most critical issue with this coding symbol is the long time window usually needed to obtain good sensitivity. The classic studies assumed that integration may rely on an arbitrarily long time window (Britten et al. 1992). However, it is questionable if individuals invest the time to reach good sensitivity in the face of a speed-accuracy trade-off. Studies focused on this issue have made it clear that animals rather decide earlier (e.g. Roitman and Shadlen, 2002). Our data tell the same story: to reach optimal sensitivity the signal needs to be

averaged over 1-2 seconds (cf. Fig 6A). Presenting similar stimuli in a reaction time task, reveals that rats typically respond within 200-300 ms, rarely waiting for repetitive pulses (Stüttgen and Schwarz 2010; Waiblinger, Brugger, and Schwarz 2015; Waiblinger, Brugger, Whitmire, et al. 2015). In our present task, however, rats were forced to experience the tactile stimulus for 4.5 s before they had a chance to lick for reward. In this case they may have utilized the longer integration time required to reach optimal sensitivity. Two hints that this may actually have happened is that, firstly, the rats in the present study, took a long time to learn the delayed task contingency (sometimes 3 months and longer). Secondly, after an extensive training procedure, focused on teaching rats to delay responding beyond the onset of tactile stimulation, the rats all learned to do the task and their psychophysical performance substantially exceeded the performance of rats which were free to respond at stimulus onset in our previous study; in fact two of those rats entirely failed to perform the task (Waiblinger, Brugger, and Schwarz 2015). Delay discounting and speed–accuracy trade-off are known strong determinants in decision making. However, trade-off balances have been shown to be adaptive and malleable in the face of differing behavioral demands (Koffarnus et al. 2013; Renda and Madden 2016), a fact that may have helped the animals in the present study to successfully perform the task by exploiting a global stimulus variable.

Spike time-locking to stimulus features is observed already in axons of the primary afferents, the very first elements of the ascending tactile pathway (Talbot et al. 1968; Deschênes et al. 2003; Jones et al. 2004; Gerdjikov et al. 2010; Chagas et al. 2013), and is inherited by all stations thereafter up to S1 (Mountcastle et al. 1969; Deschênes et al. 2003; Luna et al. 2005; Ewert et al. 2008; Petersen et al. 2008; Jadhav et al. 2009). By characterizing spike timing across a population of barrel cortex neurons, we found that sparse time-locked responses to pulsatile stimuli are even more wide-spread than hitherto thought from studies which selected neurons for rhythmic responses (Deschênes et al. 2003; Ewert et al. 2008). It is important to emphasize that tactile information contained in time-locking (Figs. 4 and 5) is not accessible by the animal without prior information about the stimulus. Therefore, for the neuronal model, we measured spike timing based on autocorrelation of spike trains. We

found a consistent mismatch in the neurometric-psychometric comparison, not based on lacking frequency information. On the contrary, neurons locked too well to the stimulus, and thus failed to give a superior fit to the rat's performance. The 15 Hz stimulus was responded to with a rhythmicity that even in the most unlikely selection of non-rhythmic pool neurons estimated the performance of neurons on average to be better than that of the animal. This surprising fact may help explain why model pools that yielded the optimal fit of frequency-based neurometric and psychometric data were much smaller as compared to the ones needed to fit the intensity-neurometric data. The fact that spike intervals contain frequency information that is far superior to what rats are able to discriminate was already seen in single primary afferents (Gerdjikov et al. 2010), and with the present insights is extended to the cortical level.

Our finding that tactile pitch information contained in timed spikes apparently cannot be used for a frequency discrimination task, resonates well with findings in the primate tactile system, where, despite the prevalence of rhythmic spiking when stimulated with sinusoidal skin deflections (Talbot et al. 1968; Mountcastle et al. 1969), rhythmicity of evoked activity was repeatedly found to be no strong requirement for frequency discrimination (Romo et al. 1998, 2000; Salinas et al. 2000). Even in the auditory system, where the cochlea acts as a spectral analyzer and pitch perception cannot be denied, the major candidate code of carrying frequency information are labeled lines (frequency maps) along which repetitive spiking vanishes and is recoded into a rate code (Rhode 1984; Micheyl et al. 2013). What, if not tactile pitch perception, is the purpose of time-locked spikes in S1? We think that the slip hypothesis, the notion that local waveform coding is used to monitor frictional stick-slip movements (Jadhav and Feldman 2010; Schwarz 2016), may provide an answer to this question. Supporting the slip hypothesis, the ascending tactile pathway conveys vast amounts of information about local variables in the vibrotactile signal (Jones et al. 2004; Arabzadeh et al. 2005; Maravall et al. 2007; Petersen et al. 2008; Jadhav et al. 2009; Stüttgen and Schwarz 2010; Chagas et al. 2013; Waiblinger, Brugger, and Schwarz 2015; McGuire et al. 2016). The prominent rhythmical engagement in response to a repetitive

tactile signal may thus be explained by the fact that the tactile system is honed to reflect details of the incoming waveform at extraordinary temporal precision. In this view, time-locked responses to a repetitive stimulus would not be generated as a means to encode frequency but as a side effect of local coding. This conclusion is compatible with a quite different form of spike timing that has been reported to occur with active whisking, namely time-locking to onset of whisker touch (Zuo et al. 2015). In contrast to time-locking to stimulus features, studied here, time-locking to touch does not appear to be suited to capture the detailed texture profile, because touch location with respect to textural elements varies with every touch. Considering however, the complex touch situation studied by these authors (e.g. smooth vs. coarsely grated surfaces, multiple whisker contacts, line contact of whiskers possibly touching several textural elements at a time, etc.) it is well conceivable that delays of the first frictional slip (accompanied by precise spiking) after touch onset may have carried significant texture information.

In summary, our comparison of global coding symbols suggests that the spike count of a pool of neurons is more adequate to capture the amount of global stimulus information used by rats, supporting its dominance over the spike timing code. From our results we posit that the occurrence and role of spike timing in primary sensory cortex can be explained in two major ways: it may either carry information about stimulus frequency before being converted to a spike count code, or be a side effect of waveform coding. While the first is likely to happen in the auditory system, the second is likely the case in the whisker-related tactile system. What might be the functional role of intensity coding as suggested here? One speculation is that it serves to supplement the dominant instantaneous code. Stick events (and with them ensuing slips) might become rare with certain surfaces or with high whisker velocities. In such cases a supplemental intensive code as demonstrated here could be highly beneficial. Future studies need to present more naturalistic stimuli, engaging the whisker in frictional movements, to shed light on the question how waveform-based and intensity-based coding schemes may work together to optimize perception.

References

Abeles M. 1982. Quantification, smoothing, and confidence limits for single- units' histograms. J Neurosci Methods. 5:317–325.

Adibi M, Diamond ME, Arabzadeh E. 2012. Behavioral study of whisker-mediated vibration sensation in rats. Proc Natl Acad Sci. 109:971–976.

Arabzadeh E, Petersen RS, Diamond ME. 2003. Encoding of whisker vibration by rat barrel cortex neurons: implications for texture discrimination. J Neurosci. 23:9146–9154.

Arabzadeh E, Zorzin E, Diamond ME. 2005. Neuronal encoding of texture in the whisker sensory pathway. PLoS Biol. 3:e17.

Batschelet E. 1981. Circular statistics in biology. London: Academic Press.

Britten KH, Shadlen MN, Newsome WT, Movshon JA. 1992. The analysis of visual motion: a comparison of neuronal and psychophysical performance. J Neurosci. 12:4745–4765.

Chagas AM, Theis L, Sengupta B, Stüttgen MC, Bethge M, Schwarz C. 2013. Functional analysis of ultra high information rates conveyed by rat vibrissal primary afferents. Front Neural Circuits. 7:190.

Delhaye B, Barrea A, Edin BB, Lefèvre P, Thonnard J-L. 2016. Surface strain measurements of fingertip skin under shearing. J R Soc Interface. 13:20150874.

Deschênes M, Timofeeva E, Lavallee P. 2003. The relay of high-frequency sensory signals in the whisker-to-barreloid pathway. J Neurosci. 23:6778–6787.

Ewert TA, Vahle-Hinz C, Engel AK. 2008. High-frequency whisker vibration is encoded by phase-locked responses of neurons in the rat's barrel cortex. J Neurosci. 28:5359–5368.

Fisher NI. 1995. Statistical analysis of circular data. Cambridge: Cambridge University

Press.

Garabedian CE, Jones SR, Merzenich MM, Dale A, Moore CI. 2003. Band-pass response properties of rat SI neurons. J Neurophysiol. 90:1379–1391.

Georgieva P, Brugger D, Schwarz C. 2014. Are spatial frequency cues used for whisker-based active discrimination? Front Behav Neurosci. 8:379.

Gerdjikov T V, Bergner CG, Stüttgen MC, Waiblinger C, Schwarz C. 2010. Discrimination of Vibrotactile Stimuli in the Rat Whisker System: Behavior and Neurometrics. Neuron. 65:530–540.

Goldberg JM, Brown PB. 1968. Functional organization of the dog superior olivary complex: an anatomical and electrophysiological study. J Neurophysiol. 31:639–656.

Green DM, Swets JA. 1966. Signal detection theory and psychophysics.

Haiss F, Butovas S, Schwarz C. 2010. A miniaturized chronic microelectrode drive for awake behaving head restrained mice and rats. J Neurosci Methods. 187:67–72.

Harris J a, Arabzadeh E, Fairhall AL, Benito C, Diamond ME. 2006. Factors affecting frequency discrimination of vibrotactile stimuli: implications for cortical encoding. PLoS One. 1:e100.

Hayward V, Terekhov A V, Wong S, Geborek P, Bengtsson F, Jörntell H. 2014. Spatio-temporal skin strain distributions evoke low variability spike responses in cuneate neurons. J R Soc Interface. 11:20131015.

Hermle T, Schwarz C, Bogdan M. 2004. Employing ICA and SOM for spike sorting of multielectrode recordings from CNS. J Physiol Paris. 98:349–356.

Jadhav SP, Feldman DE. 2010. Texture coding in the whisker system. Curr Opin Neurobiol. 20:313–318.

Jadhav SP, Wolfe J, Feldman DE. 2009. Sparse temporal coding of elementary tactile

features during active whisker sensation. Nat Neurosci. 12:792–800.

Johansson RS, Birznieks I. 2004. First spikes in ensembles of human tactile afferents code complex spatial fingertip events. Nat Neurosci. 7:170–177.

Jones LM, Depireux DA, Simons DJ, Keller A. 2004. Robust temporal coding in the trigeminal system. Science (80-). 304:1986–1989.

Jörntell H, Bengtsson F, Geborek P, Spanne A, Terekhov A V., Hayward V. 2014. Segregation of tactile input features in neurons of the cuneate nucleus. Neuron. 83:1444–1452.

Khatri V, Hartings JA, Simons DJ. 2004. Adaptation in Thalamic Barreloid and Cortical Barrel Neurons to Periodic Whisker Deflections Varying in Frequency and Velocity. J Neurophysiol. 92:3244–3254.

Koffarnus MN, Jarmolowicz DP, Mueller ET, Bickel WK. 2013. Changing delay discounting in the light of the competing neurobehavioral decision systems theory: a review. J Exp Anal Behav. 99:32–57.

LaMotte RH, Mountcastle VB. 1975. Capacities of humans and monkeys to discriminate vibratory stimuli of different frequency and amplitude: a correlation between neural events and psychological measurements. J Neurophysiol. 38:539–559.

Lederman SJ. 1982. The perception of texture by touch. In: Schiff W,, Foulke E, editors. Tactual perception: A sourcebook. Cambridge: Cambridge University Press. p. 130–167.

Luna R, Hernandez A, Brody CD, Romo R. 2005. Neural codes for perceptual discrimination in primary somatosensory cortex. Nat Neurosci. 8:1210–1219.

Mackevicius EL, Best MD, Saal HP, Bensmaia SJ. 2012. Millisecond precision spike timing shapes tactile perception. J Neurosci. 32:15309–15317.

Maravall M, Petersen RS, Fairhall AL, Arabzadeh E, Diamond ME. 2007. Shifts in coding properties and maintenance of information transmission during adaptation in barrel cortex. PLoS Biol. 5:e19.

Marr D. 1982. Vision. A computational investigation into the human representation and processing of visual information. New York: Freeman.

McGuire LM, Telian G, Laboy-Juárez KJ, Miyashita T, Lee DJ, Smith KA, Feldman DE. 2016. Short time-scale sensory coding in S1 during discrimination of whisker vibrotactile sequences. PLOS Biol. 14:e1002549.

Melzer P, Sachdev RN, Jenkinson N, Ebner FF. 2006. Stimulus frequency processing in awake rat barrel cortex. J Neurosci. 26:12198–12205.

Micheyl C, Schrater PR, Oxenham AJ. 2013. Auditory frequency and intensity discrimination explained using a cortical population rate code. PLoS Comput Biol. 9:e1003336.

Möck M, Butovas S, Schwarz C. 2006. Functional unity of the ponto-cerebellum: evidence that intrapontine communication is mediated by a reciprocal loop with the cerebellar nuclei. J Neurophysiol. 95:3414–3425.

Mountcastle VB, Talbot WH, Sakata H, Hyvarinen J. 1969. Cortical neuronal mechanisms in flutter-vibration studied in unanesthetized monkeys. Neuronal periodicity and frequency discrimination. J Neurophysiol. 32:452–484.

Petersen RS, Brambilla M, Bale MR, Alenda A, Panzeri S, Montemurro MA, Maravall M. 2008. Diverse and temporally precise kinetic feature selectivity in the VPm thalamic nucleus. Neuron. 60:890–903.

Renda CR, Madden GJ. 2016. Impulsive choice and pre-exposure to delays: III. Four-month test-retest outcomes in male wistar rats. Behav Processes. 126:108–112.

Rhode WS. 1984. Cochlear mechanics. Annu Rev Physiol. 46:231–246.

Roitman JD, Shadlen MN. 2002. Response of Neurons in the Lateral Intraparietal Area during a Combined Visual Discrimination Reaction Time Task. J Neurosci. 22:9475–9489.

Romo R, Hernandez A, Zainos A, Brody CD, Lemus L. 2000. Sensing without touching: psychophysical performance based on cortical microstimulation. Neuron. 26:273–278.

Romo R, Hernandez A, Zainos A, Salinas E. 1998. Somatosensory discrimination based on cortical microstimulation. Nature. 392:387–390.

Salinas E, Hernandez A, Zainos A, Romo R. 2000. Periodicity and firing rate as candidate neural codes for the frequency of vibrotactile stimuli. J Neurosci. 20:5503–5515.

Schwarz C. 2016. The slip hypothesis: Tactile perception and its neuronal bases. Trends Neurosci. 39:449–462.

Schwarz C, Hentschke H, Butovas S, Haiss F, Stüttgen MC, Gerdjikov T, Bergner C, Waiblinger C. 2010. The head-fixed behaving rat - procedures and pitfalls. Somatosens Mot Res. 27:131–148.

Stanislaw H, Todorov N. 1999. Calculation of signal detection theory measures. Behav Res Methods Instrum Comput. 31:137–149.

Stüttgen MC, Rüter J, Schwarz C. 2006. Two psychophysical channels of whisker deflection in rats align with two neuronal classes of primary afferents. J Neurosci. 26:7933–7941.

Stüttgen MC, Schwarz C. 2008. Psychophysical and neurometric detection performance under stimulus uncertainty. Nat Neurosci. 11:1091–1099.

Stüttgen MC, Schwarz C. 2010. Integration of vibrotactile signals for whisker-related perception in rats is governed by short time constants: comparison of neurometric and psychometric detection performance. J Neurosci. 30:2060–2069.

Stüttgen MC, Schwarz C, Jäkel F. 2011. Mapping spikes to sensations. Front Neurosci. 5:1–

17.

Talbot WH, Darian-Smith I, Kornhuber HH, Mountcastle VB. 1968. The sense of flutter-vibration: comparison of the human capacity with response patterns of mechanoreceptive afferents from the monkey hand. J Neurophysiol. 31:301–334.

Waiblinger C, Brugger D, Schwarz C. 2015. Vibrotactile discrimination in the rat whisker system is based on neuronal coding of instantaneous kinematic cues. Cereb Cortex. 25:1093–1106.

Waiblinger C, Brugger D, Whitmire CJ, Stanley GB, Schwarz C. 2015. Support for the slip hypothesis from whisker-related tactile perception of rats in a noisy environment. Front Integr Neurosci. 9:53.

Wolfe J, Hill DN, Pahlavan S, Drew PJ, Kleinfeld D, Feldman DE. 2008. Texture coding in the rat whisker system: slip-stick versus differential resonance. PLoS Biol. 6:e215.

Yoshioka T, Gibb B, Dorsch a K, Hsiao SS, Johnson KO. 2001. Neural coding mechanisms underlying perceived roughness of finely textured surfaces. J Neurosci. 21:6905–6916.

Zuo Y, Safaai H, Notaro G, Mazzoni A, Panzeri S, Diamond ME. 2015. Complementary contributions of spike timing and spike rate to perceptual decisions in rat S1 and S2 cortex. Curr Biol. 25:357–363.

Figure legends

Fig. 1: Behavior paradigm and psychophysical performance. **A:** Illustration of the behavioral task. **B:** Psychophysical performance. Response probabilities plotted for each of the three animals (levels of gray) tested in the task. **C:** Same data but plotted as area under ROC curve (AUC) averaged across rats. Random performance (AUC = 0.5) is marked with a dashed line. Animals successfully discriminated lower frequencies from the 90 Hz stimulus. Error bars are 0.05-0.95 confidence intervals based on a binomial distribution.

Fig. 2: Spike response to pulsatile stimuli. **A:** Example raster displays, PSTHs and cumulative spike counts of barrel cortex units that were excited (upper panel), inhibited (lower panel) or whose firing rate was unchanged (middle panel) by tactile stimulation. Neuron numbers refer to units marked in B and C. **B:** Relationship between baseline firing rate and evoked firing rate as obtained from the last 4s of the stimulus period. **C:** Excess spikes (based on Poisson firing model) of all units recorded in the current experiment averaged across all stimulation frequencies.

Fig. 3. Frequency tuning. **A:** Tuning curves for the 80 single units in the sample (gray lines). The median and [25% 75%] percentiles are shown as full and broken black lines respectively. **B:** Number of spikes per pulse for each frequency tested (the box shows median and interquartile ranges; whisker length: 1.5 x interquartile range; crosses mark outliers).

Fig. 4: Spike timing in response to pulsatile stimuli. PSTH and phase histograms for two example neurons that did not change firing rates in response to the stimulus (different from the one shown in Fig. 2). Neuron 1 displays good time locking to the stimulus pulses, while neuron 2 does not. The inset for neuron 1 shows three example spikes relative to stimulus pulse onsets during the first presentation of the 30 Hz stimulus.

Fig. 5: Time locking in the recorded population of units. **A:** Plot of frequency of latencies of peak response for the total sample of neurons (N=80). The response is locked to absolute time – not the phase of pulse frequency. With 75 and 90 Hz stimuli a spill-over of time-locked spikes into the next stimulus period is observed. **B:** Vector strength of all neurons plotted against excess spikes (only responses to 15 Hz stimuli are shown). Vector strength would assume one if all spikes were contained in one bin of the phase histogram, and zero for a flat distribution. Excess spikes indicate evoked firing based on a Poisson firing model (negative = evoked suppression of spiking). High locking is observed predominantly with non-responding and excited cells. Black circles indicate significant vector strengths (Raleigh test, $p<0.05$; open circles: $p>0.05$). **C:** Normalized vector strength of the total sample of cells. As the stimulus is non-sinusoidal, the different pulsatile stimuli by themselves show different vector strengths. Therefore we related the measured vector strength of spiking to that obtained with spiking to the 15 Hz stimulus, but using the periods of the other frequencies. This measure is expected to assume one if time locking survives higher frequency stimulation. At the highest frequencies (75, 90) the normalized vector strength has the tendency to decrease. This is likely due to spill over of time-locked spikes into the next inter-pulse period.

Fig. 6: Sensitivity based on spike counts. **A:** Sensitivity (AUC) based on spike count distributions obtained from windows with increasing duration (three example units, levels of gray). **B:** Histograms of sensitivities observed in the total sample. Spike counts obtained with varying window durations are plotted in different shades of gray. Progressively darker curves represent neurometric performance and windows of 30 to 125 – 5000 ms (excluding the on-response by omitting the first 30 ms) and the on-response itself (window 0-50 ms; broken line). Psychophysical sensitivity is replotted for comparison (arrows pointing to the mean AUC values, same data as shown in Fig. 1C).

Fig. 7: Comparison between psychometric and neurometric performance based on simulated PSTHs derived from neuronal pools of various size (3-160) and composition (i.e., rank ordered response quality, 10-80 best neurons). Best-responding neurons were taken to be the neurons showing the highest number of excess spikes (top: intensity code) or highest vector strengths (bottom: frequency code) for 60Hz stimulation. **Top:** Spike count code. Difference of spike-count-based neurometric performance (full stimulus interval) and psychometric performance plotted as Euclidean distance (ED) for all parameter combinations (matrix, most similar is blue, most dissimilar is red). Three examples of resulting neurometric curves (blue) are shown. The psychometric curve is replotted (red) in each graph to ease comparison. The best model found (minimum ED) is highlighted by the gray background. **Bottom:** Same for time-locking. Note that the neurometric variable is based on rhythmicity obtained from population PSTHs and not from measures of vector strength (the latter is not accessible for the brain without prior knowledge about stimulus phase).

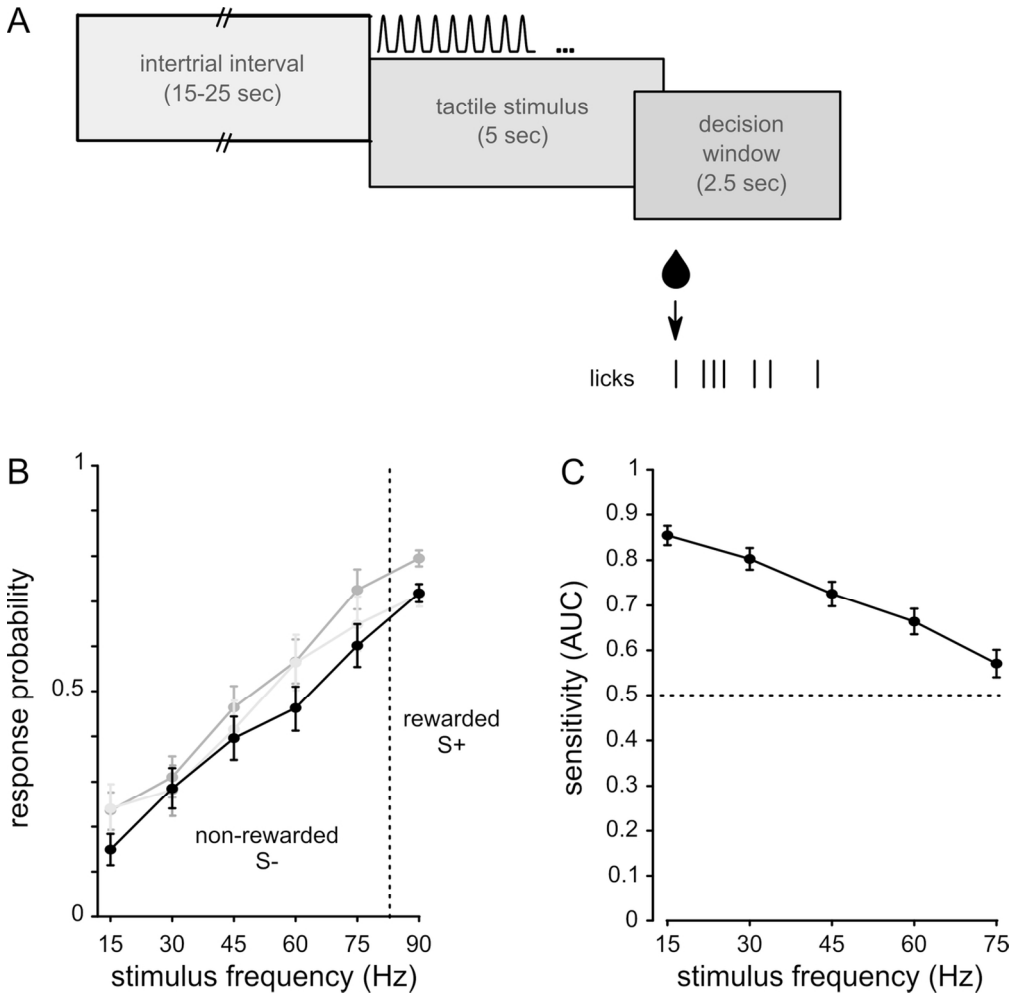

Fig. 1: Behavior paradigm and psychophysical performance. A: Illustration of the behavioral task. B: Psychophysical performance. Response probabilities plotted for each of the three animals (levels of gray) tested in the task. C: Same data but plotted as area under ROC curve (AUC) averaged across rats. Random performance (AUC = 0.5) is marked with a dashed line. Animals successfully discriminated lower frequencies from the 90 Hz stimulus. Error bars are 0.05-0.95 confidence intervals based on a binomial distribution.

119x117mm (300 x 300 DPI)

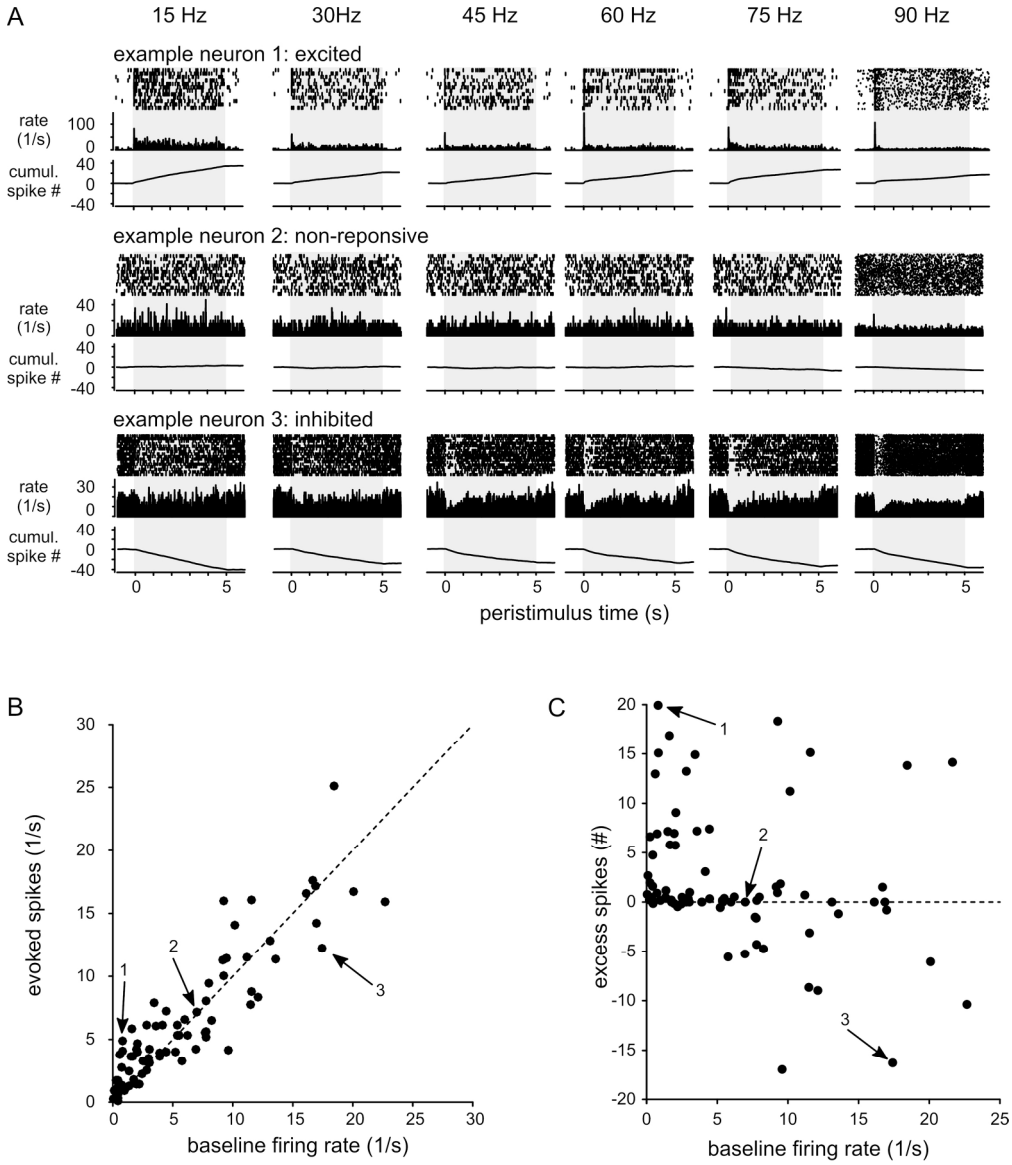

Fig. 2: Spike response to pulsatile stimuli. A: Example raster displays, PSTHs and cumulative spike counts of barrel cortex units that were excited (upper panel), inhibited (lower panel) or whose firing rate was unchanged (middle panel) by tactile stimulation. Neuron numbers refer to units marked in B and C. B: Relationship between baseline firing rate and evoked firing rate as obtained from the last 4s of the stimulus period. C: Excess spikes (based on Poisson firing model) of all units recorded in the current experiment averaged across all stimulation frequencies.

192x221mm (300 x 300 DPI)

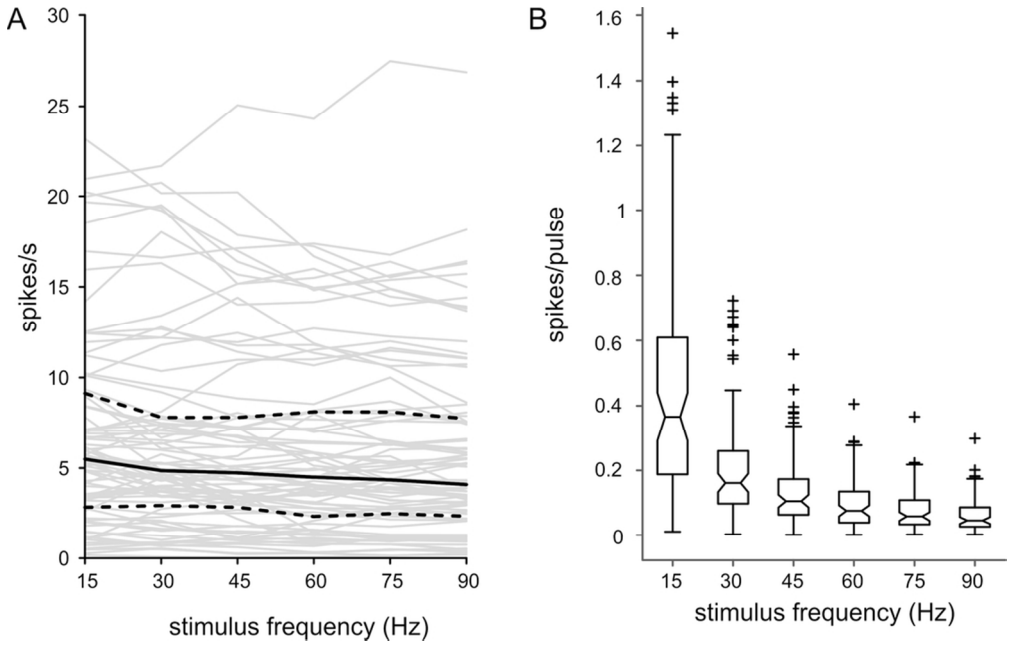

Fig. 3. Frequency tuning. A: Tuning curves for the 80 single units in the sample (gray lines). The median and [25% 75%] percentiles are shown as full and broken black lines respectively. B: Number of spikes per pulse for each frequency tested (the box shows median and interquartile ranges; whisker length: 1.5 x interquartile range; crosses mark outliers).

90x56mm (300 x 300 DPI)

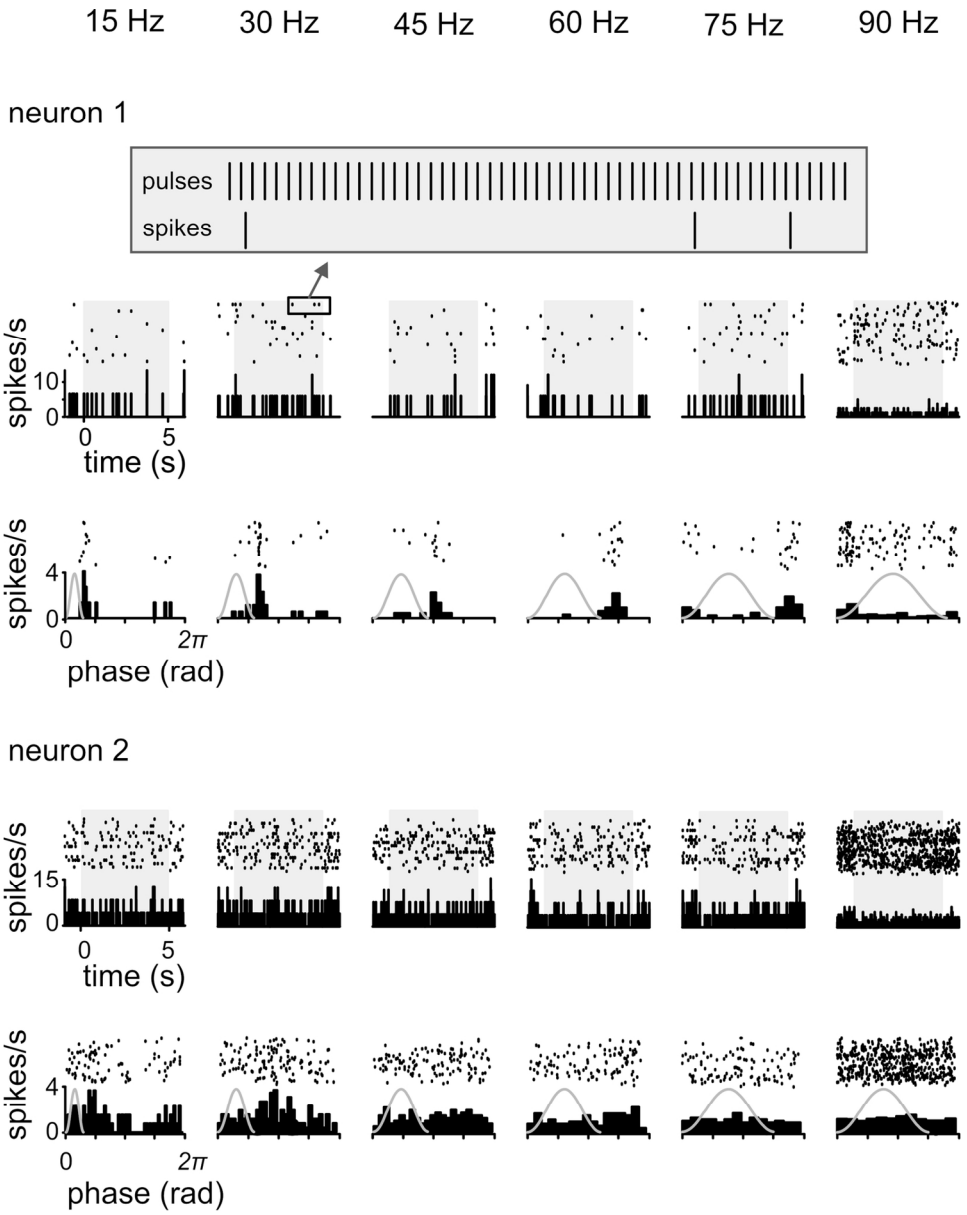

Fig. 4: Spike timing in response to pulsatile stimuli. PSTH and phase histograms for two example neurons that did not change firing rates in response to the stimulus (different from the one shown in Fig. 2). Neuron 1 displays good time locking to the stimulus pulses, while neuron 2 does not. The inset for neuron 1 shows three example spikes relative to stimulus pulse onsets during the first presentation of the 30 Hz stimulus.

137x172mm (300 x 300 DPI)

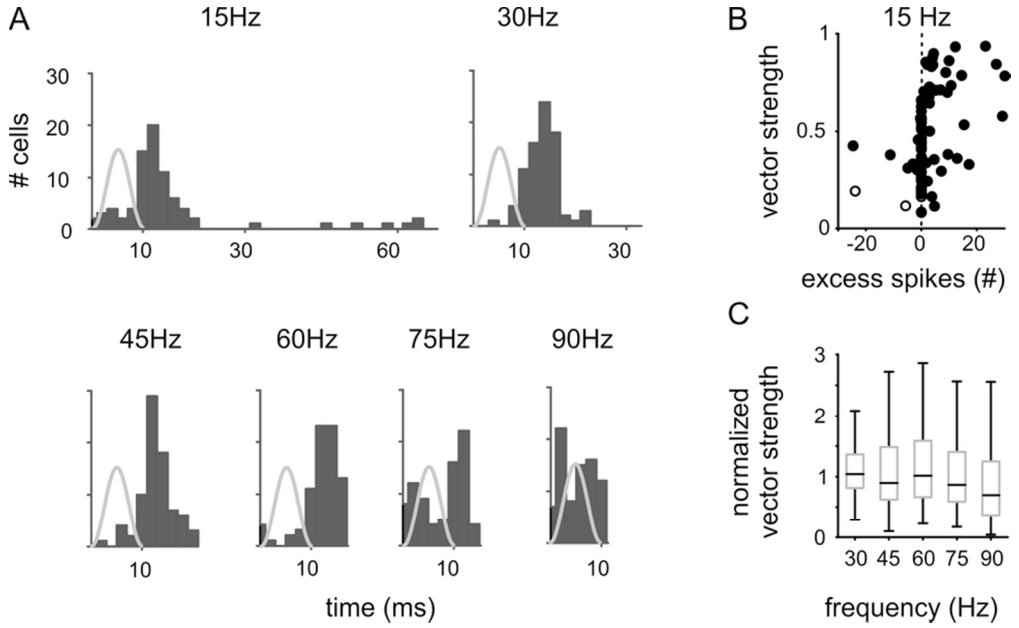

Fig. 5: Time locking in the recorded population of units. A: Plot of frequency of latencies of peak response for the total sample of neurons (N=80). The response is locked to absolute time – not the phase of pulse frequency. With 75 and 90 Hz stimuli a spill-over of time-locked spikes into the next stimulus period is observed. B: Vector strength of all neurons plotted against excess spikes (only responses to 15 Hz stimuli are shown). Vector strength would assume one if all spikes were contained in one bin of the phase histogram, and zero for a flat distribution. Excess spikes indicate evoked firing based on a Poisson firing model (negative = evoked suppression of spiking). High locking is observed predominantly with non-responding and excited cells. Black circles indicate significant vector strengths (Raleigh test, $p<0.05$; open circles: $p>0.05$). C: Normalized vector strength of the total sample of cells. As the stimulus is non-sinusoidal, the different pulsatile stimuli by themselves show different vector strengths. Therefore we related the measured vector strength of spiking to that obtained with spiking to the 15 Hz stimulus, but using the periods of the other frequencies. This measure is expected to assume one if time locking survives higher frequency stimulation. At the highest frequencies (75, 90) the normalized vector strength has the tendency to decrease. This is likely due to spill over of time-locked spikes into the next inter-pulse period.

82x50mm (300 x 300 DPI)

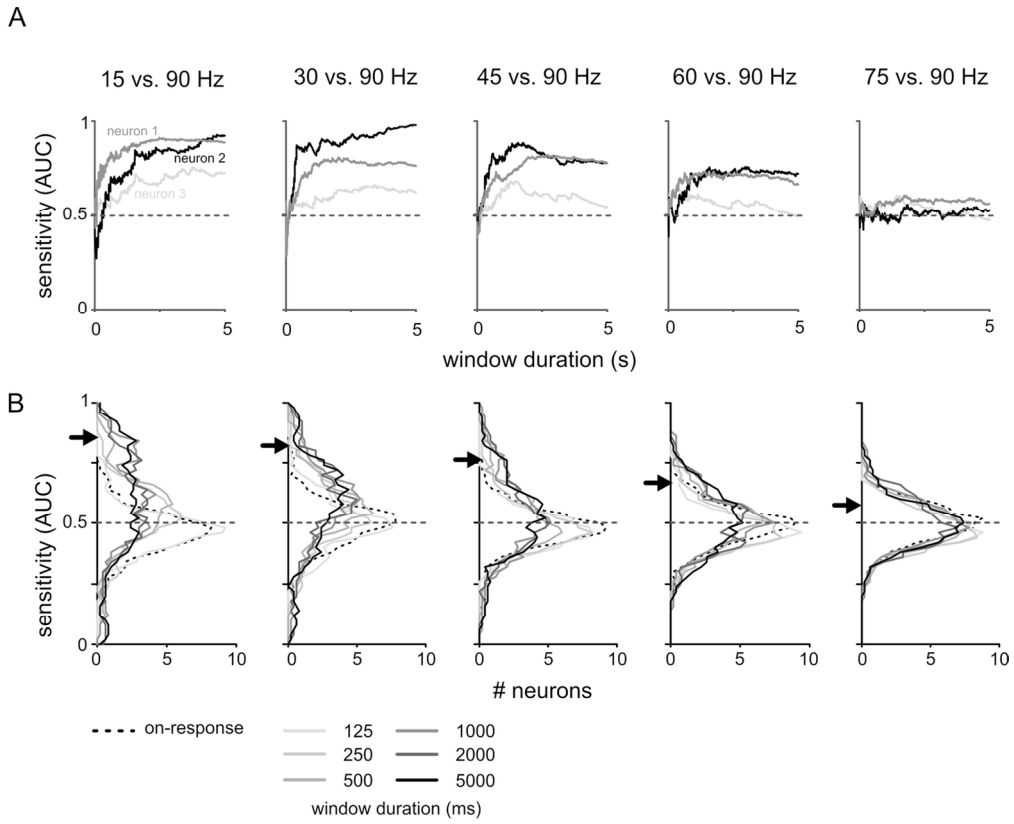

Fig. 6: Sensitivity based on spike counts. A: Sensitivity (AUC) based on spike count distributions obtained from windows with increasing duration (three example units, levels of gray). B: Histograms of sensitivities observed in the total sample. Spike counts obtained with varying window durations are plotted in different shades of gray. Progressively darker curves represent neurometric performance and windows of 30 to 125 – 5000 ms (excluding the on-response by omitting the first 30 ms) and the on-response itself (window 0-50 ms; broken line). Psychophysical sensitivity is replotted for comparison (arrows pointing to the mean AUC values, same data as shown in Fig. 1C).

128x104mm (300 x 300 DPI)

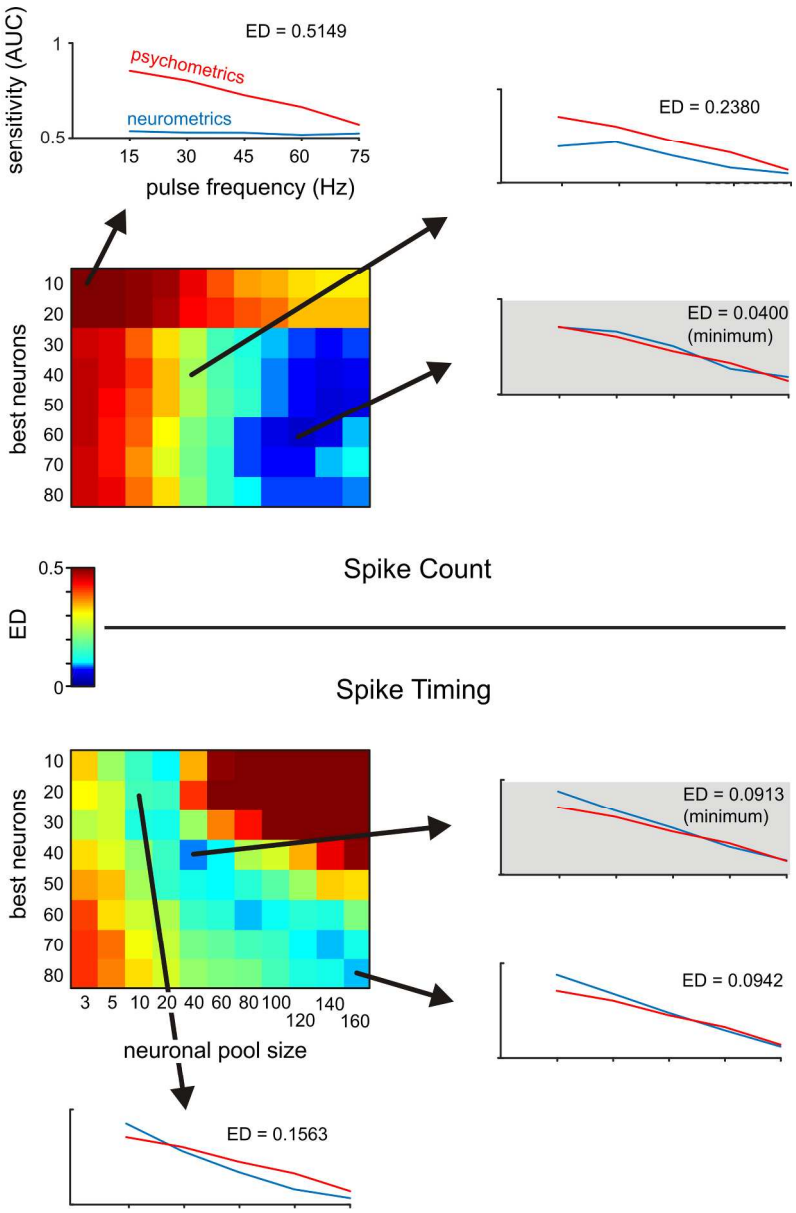

Fig. 7: Comparison between psychometric and neurometric performance based on simulated PSTHs derived from neuronal pools of various size (3-160) and composition (i.e., rank ordered response quality, 10-80 best neurons). Best-responding neurons were taken to be the neurons showing the highest number of excess spikes (top: intensity code) or highest vector strengths (bottom: frequency code) for 60Hz stimulation. Top: Spike count code. Difference of spike-count-based neurometric performance (full stimulus interval) and psychometric performance plotted as Euclidean distance (ED) for all parameter combinations (matrix, most similar is blue, most dissimilar is red). Three examples of resulting neurometric curves (blue) are shown. The psychometric curve is replotted (red) in each graph to ease comparison. The best model found (minimum ED) is highlighted by the gray background. Bottom: Same for time-locking. Note that the neurometric variable is based on rhythmicity obtained from population PSTHs and not from measures of vector strength (the latter is not accessible for the brain without prior knowledge about stimulus phase).

187x282mm (300 x 300 DPI)